GROUND PENETRATING RADAR (GPR) SURVEY ON THE LAVA FLOW IN THE SUBANG AREA, WEST JAVA PROVINCE, INDONESIA

Hendarmawan[*)]
Laboratorium Geologi Lingkungan & Hidrogeologi, Fakultas Teknik Geologi, UNPAD
***)** Email: hendarmawan.@unpad.ac.id

ABSTRACT

Most hydrogeologist often meet the difficulties for exploration on tle lava flow when groundwater flow within that channel not emerging or no sputed on the surface. While, in other view, depending on frequency, GPR can resolve objects down to the size of a few meters or even centimeters, and this geophysical reflection method with the highest resolving power (GPR) is also as well established tool for geophysical investigations of the shallow subsurface. Thus, it is not surprising if this approach is used at lava flow terrain, in the Subang area. The tim can directly recognized the secondary permeable zone to recommendate the icline drilling with high accurate. Therefore, in this case, the extra effort and cost involved exceed the maksimum benefits or effisien.

***Keywords**: groundwater exploration, lava flow, fracture zones, drilling, groundwater discharge*

ABSTRAK

Para ahli hidrolgeologi seringkali menemui kesulitan untuk eksplorasi di aliran lava saat airtanah yang mengalir dalam saluran tidak muncul atau tidak dibahas di permukaan. Sementara dalam pandangan lain, tergantung frekuensi, GPR dapat menjelaskan objek ke ukuran beberapa meter atau bahkan centimeter, dan metode refleksi geofisika ini dengan berkekuatan penyelesaian tertinggi (GPR) adalah juga sebagai alat mapan untuk penyelidikan geofisika dari bawah permukaan yang dangkal. Jadi, tidak mengherankan jika pendekatan ini digunakan pada daerah aliran lava di daerah Subang. Tim ini langsung bisa mengenal zona permeabel sekunder untuk rekomendasi pengeboran miring dengan akurasi tinggi. Oleh karena itu, dalam kasus ini, upaya ekstra dan biaya yang terlibat melebihi manfaat maksimum atau efisien.

Kata kunci: eksplorasi air tanah, aliran lava, zona fraktur, pengeboran, debit air tanah

INTRODUCTION

GPR is a fast and non-destructive method and the data is often interpreted without any processing, since in many cases the extra effort and cost involved exceed the benefits. Depending on frequency, GPR can resolve objects down to the size of a few meters or even centimeters, and is, therefore, the geophysical reflection method with the highest resolving power. Thus, it is not surprising that Ground Penetrating Radar (GPR) is a well established tool for geophysical investigations of the shallow subsurface. This makes GPR a financially attractive alternative to shallow seismic exploration methods and also popular with many professionals in many field such as environmental and engineering geophysics including hydrogeological field.

For specific applications GPR data processing is performed to increase the lateral and vertical resolution and to determine the velocity model with higher accuracy. The processing applied to GPR data can be broken down into two groups:

- Standard data processing utilizing the whole range of seismic data processing techniques.These are usually situations where the scientific, environmental or financial benefits exceed the extra cost involved. For example, CMP measurements, velocity analyses and migration are performed in the same way as for seismic data.
- Specialized data processing. These applications are more numerous than in seismic data processing. GPR data processing is used in a

wide range of problems, e.g. in the detection of pipes and cables, the assessment of cavities or fracture behind tunnel lining, and the automatic detection of obstacles for tunneling machines

The work presented here is concerned with a problem from the second group, namely, the development of techniques to extract characteristic parameters of targets from single offset GPR data. The parameters, e.g. velocity, amplitudes and time-lag between reflections, are then utilized to distinguish between three target materials: air, water and soil/stone. The identification of target materials is based on the dielectric constants obtained from velocities or reflection coefficients (via amplitudes). In a second step, the vertical size of the target is calculated from the dielectric constant and the time-lag between intra-target reflections. For many applications it is sufficient to be able to distinguish the responses of cavities from those of other reflections. Here are some possible applications:

- For safety and financial reasons the quality of concrete or the degree of erosion below runways and roads has to be assessed.
- In karstic/vulcanic areas planned building sites have to be secured by injecting concrete into cavities.
- Old water-delivery tunnels can become leaky, wash out cavities and cause great loss of water.
- In archeology the location and state of preservation of tombs may be of interest.

The purpose of this study is to assess the feasibility of the structural and hydrogeological characteristics using ground penetrating radar on the Pasawahan Spring area of PT. Tirta Investama, Subang Distric, West Java.

BASIC THEORY

In this study, a RAMAC MALA GEOSIENCE GPR system (Table 1), consisting of a transmitting and receiving antenna connected to a console and laptop computer (Fig. 1), was used. The transmitted electromagnetic pulse is ideally meant to penetrate the subsurface in a beam as narrow as possible. Some of the energy, however, travels directly to the receiving antenna as air-wave and ground-wave, giving the signal at the top of the resulting radar section (Fig. 1). Part of the remaining energy, which enters the subsurface, reflects at layers of changing dielectric impedance and travels back to the receiver. The quantity of energy received and the associated arrival time are stored in the computer. The lateral extent and morphology of reflectors can be delineated by moving the portable equipment across the surface. The resulting radar section, on which each measurement point is represented by a trace, shows time along its vertical axis and position along its horizontal axis.

The relative permittivity (εr), which is mainly controlled by water content, is the most important parameter governing the reflection process and wave velocity (Table 1). When a significant change in relative permittivity is encountered, part of the electromagnetic energy is reflected, the reflection being proportional to the magnitude of change. For most materials, the relative magnetic permeability (μ) is near unity. Consequently, the magnetic permeability in the subsurface is near the free-space value and plays no role in the electromagnetic energy behaviour. However, under certain conditions, such as the presence of iron and iron oxides, relative magnetic permeability can be enhanced significantly (Von Hippel, 1954; Olhoeft & Capron, 1994). The electrical conductivity of a material influences penetration depth as well as resolution. Low-conductivity materials, such as unsaturated and coarse-grained sediments, cause little attenuation and, under ideal circumstances, penetration is of the order of tens of metres (Davis & Annan, 1989) (Table 1). However, wave velocity and length are highest in low-conductivity materials, leading to a decrease in resolution (Table 2). Penetration depth and resolution are also influenced by the GPR frequency used for measurement. Lower antenna frequencies are favourable for greater penetration, but result in a decrease in resolution. Resolution is approximately a quarter of the GPR wavelength, and ranges from 0,05 m for saturated sands and 200-MHz antennas to 0,5 m for dry sands and 100-MHz antennas (Table 2).

Table showing how to select Antenna Frequency, all values entered in these tables are empiric and approximative. They may therefore not necessarily correspond to theoretically calculated.

The following table gives approximate values for εr (relative permittivity) and the resulting velocities for a number of medias. ervaries greatly with the water content in the medium. The larger value given for a velocity applies to a more unsaturated media.

METHODOLOGY

Test site and experimental lay out

This experiment was conducted around the water spring of PT. TIRTA INVESTAMA, Subang, West Jawa in 10 December 2006. A wet lava-andecit rock boulder with fracture found at the site. Then it was determined from GPR survey that the near-surface stratigraphic structure consists of a 5-10-m thick layer of lava andecit aquifer material. Near pumping station/Rumah Sumber area was relatively flat land and the selected lines area was mainly bare with some concrete. A plan view of the experimental layout is shown in Figure 3 and 4. There are 11 GPR survey lines were running near pumping station/rumah sumber area, 6 lines were collected by 100 MHz antenna (SBLA code), and 5 others by 50 MHz antenna (SBLB code).

GPR data collection

A RAMAC MALA GEOSCIENCE unit with 50 and 100 MHz antennas was used. GPR data were acquired by shooting a single-fold common offset line along the artificial ledge forming the top of the vertical face.

Acquisition parameters included 100 MHz and 50 MHz antennas, source/ receiver offset of 1 m and 2 m, midpoint interval of 0.5 m and 1 m, time sample rate of 0.8 nanoseconds and a 256-fold vertical stack. With a three-person team, acquisition time from first to last shot was 60-90 minutes.

The raw data are show in Figure 4 with 10 ns of dewow and no display gain. Note the time scale, is in nanoseconds. Lateral extent of the line is coincident with the drawing in Figure 3. The raw data are dominated by direct arrivals at 10-40 ns or 0.5 – 1 m. The relative strength of reflections on this part of the line is a qualitative measure of fresh rock saturated by groundwater. Observed conditions of the rock face in this vicinity support the interpretation of heavier weathering. For a hydrogeology this would provide an important indication of rock competency. This is energy reflected from the altered region in the vicinity of a fracture.

GPR data processing

Beginning with the raw GPR data, considerable processing is required to produce a final image. All data display and processing for the GPR data was accomplished using ReflexW and SU (Seismic Unix) public-domain processing system maintained by the

Center for Wave Phenomena, Colorado School of Mines.

Our standard processing stream for high-quality GPR data is low-cut filter (O-20 MHz), time shift to t-zero, NMO, DMO, and migration. Low-cut filtering removes DC amplitudes resulting from system "wow" (low frequency, periodic interference). The t-zero shift is required because t = 0 on the raw data does not correspond to source-initiation time. To correct to source time, t = 0 is determined from first-arrival time minus 20-30 ns and the data is given a static shift to this t-zero. NM0 and DMO account for finite offset in the data to produce a zero offset section, while preserving all dipping events. Every data set was processed with exactly the same parameters :

- Noise removal
- First arrival alignment
- Empty data-set subtraction
- Bandpass filter: Butterworth 50–100 1500–2000 MHz
- AGC
- Stolt three-dimensional migration
- Radon transform (ϑ-p) filtering
  Time to depth conversion

RESULTS AND DISCUSSION

Signal Result of GPR Survey

Survey results are presented in figures 5 and 6. Again, the horizontal axis on all ground penetrating radar (GPR) profiles represents distance in meters (m) along the transect line where measurements were obtained. The left vertical axis on all profiles gives depth section in meter (ns). Both vertical and horizontal axes on GPR amplitude maps give distance in meters (m).

Figure 5 shows the GPR SBLA lines response from 100 MHz antenna frequencies. All the GPR data for Figure 5 were collected at the upper part along tha village road (figure 03) survey under dry and hot weather conditions, a station interval of 5 cm, and a signal trace stacking of 4. Figures 5a-5f obtained using a RAMAC/GPR unit with 100 MHz center frequency antennas. A laterally high amplitude feature is the typical GPR wet soil/rock response shown on profiles, obtained from measurements collected along a transect perpendicular to the trend of a groundwater line flow prediction. The high amplitude beneath surface, referred to as "hot spot" by geophysicists, denotes the actual position of water present. The high amplitude response to groundwater saturated zone to a greater or lesser extent in figures 5a-5f at depth vary between 1 to 10 m.

Figure 6 (6a-6e) depicts the GPR SBLB lines response from 50 MHz antenna frequencies. All the GPR data for Figure 6 also were collected at near area of Pumping Station/Rumah Sumber. Survey still under dry and hot weather conditions, a station interval of 10 cm, and a signal trace stacking of 4. Figures 6a-6e were obtained using a RAMAC/GPR unit with 50 MHz center frequency antennas.

Interpretation of Hydrogeological Setting

Interpretation of GPR Result Profiles:

- In the GPR data from line SBLA1-SBLA6, fault/fracture-related structures are seen clearly as terminations of laterally continuous reflections and apparent vertical offsets. In Figure 5a-5f, an interpreted GPR section is compared. The GPR section shows a principal and two secondary traces of the fracture/fault. The results correlate well with corresponding observations in the outcrop. However, the horizontal and vertical location of the fracture/Fault in the shallow subsurface is clearly imaged in the GPR data.
  The results obtained at the known fracture/fault provided a template

or pattern to seek in relation to potential fracture elsewhere along the profiles. At the known fracture (Figure 5a and 5c) the radar data reveal a strong amplitude reflection at the side of the lava-andecit layer. The significant changes in dielectric constant at the fracture (i.e., between fresh rock and the water of the fracture and between the water of the fracture and the soil beneath) cause strong radar reflections.
Anomalies also were observed in the data that were not related to fracture, but instead associated with both underground and above ground features. These included groundwater lines, fresh-rock boulder, and another subsurface material. However, each of these anomalies could be related to an observed feature and identified as such.

- Regarding figure 6, A laterally high amplitude feature is the typical GPR wet soil/rock response shown on profiles, obtained from measurements collected along a transect perpendicular to the trend of a groundwater line flow prediction. The high amplitude, referred to as "hot spot" by geophysicists, denotes the actual position of water table present. The high amplitude response to groundwater saturated zone to a greater or lesser extent in figures 6a-6e at depth vary between 5 to 20 m.

Interpretation of water bearing capacity:

- SBLA1 line suggests that tuff lapilli layer covers the area from the topsoil until about 4 m deep. It is clear that there are two boulder bodies on the left and the middle part. While, the fractures with water saturated possibly are developed at the boulder on the left part adjacent to the other in around 10 m from starting line with 4 and 9 or 10 m deep.
- At the SBLA2 line, Zone with water saturated may be identified at 7.5 m from starting survey line with 9 or 10 m deep. Two boulders are shown at 7 m deep.
- The fractures with saturated of water are probably existing at 10 m from starting line and about 5 deep on the SBLA3 line.
- At the SBLA4 line and the SBLA5 line, laterally continuous reflections indicate rock layers, while a strong amplitude indicates boulder. The white reflections may possible be fracture systems, in particular around 15 m from starting line at deep of 8-10 m (SBLA4 line) and around 17 m from starting line at deep of 7-9 m (SBLA5 line).
- At the SBLA 6, boulder with fracture system develops and indicates possibly water table at 9 meter deep.
- Generally all of interpretation of GPR data (radargram) shows us, there are 3-4 subsurface layers, until 11-12 m depth for 100 MHz antenna and 19-20 m depth for 50 MHz antenna. The first layer with 0-2 m depth interpreted to top soil (tuff)/concrete, second layer with less then 12 m, interpreted to volcanic tuff with lava-andecit as bed rock, and third layer interpreted to solid breccia with boulder.

CONCLUSIONS

Groundwater Flow System

- At least 2 groundwater flow systems developed that is flow path onto the eastern part and western part with the boundary around middle up to the end of SBLA3 line.
- On the eastern part the groundwater flow system indicated in the fracture system.
- On the western part, the groundwater flow system indicated

not only developing in the fractures systems but also the layers with water saturated.

Recommendation

Drilling points are executed as the following locations:

- Located at 10 meter from starting SBLA1 line, but the water level may be not positive, exception if drilling no vertical.
- Located at 9 meter from starting SBLA2 line
- Located at 10.5 meter from starting SBLA3 line
- Located at 15 meter from starting SBLA4 line
- Located at 18 meter from starting SBLA5 line
- Located at 4 meter from starting SBLA6 line

REFFERENCES

Allred, B. J., N. R. Fausey, L. Peters, Jr., C. Chen, J. J. Daniels, H. Youn. *In review. Detection of buried agricultural drainage pipe using conventional geophysical methods*. Submitted to Transactions of the ASAE.

Chen, H., H.H. Xu, and Y. Hu. 1991. Detecting underground cables and metal conducting pipes using EM methods. In: *Investigations in Geophysics No. 5, Geotechnical and Environmental Geophysics, V. 3, Geotechnical*. S. Ward, Editor. Soc. Exploration Geophysicists. Tulsa, UK, pp. 229-237.

Conyers, L.B. and D. Goodman. 1997. *Ground-Penetrating Radar: An . Introduction for Archaeologists Walnut Creek, California*. AltaMira Press. 232 pages.

Hayakawa, H. and A. Kawanaka. 1998. Radar imaging of underground pipes by automated estimation of velocity distribution versus depth. *J. Applied Geophysics. vol. 40, pp. 37-48.*

LaFaleche, P.T. J.P. Todoeschuck, O.G. Jensen, and A.S. Judge. 1991. Analysis of ground probing radar data: Predictive deconvolution. *Canadian Geotechnical J. v. 28, no. 1, pp. 134-139.*

Peters, Jr., L., and J.D. Young. 1986. Applications of subsurface transient radar. In: *Time Domain Measurements in Electromagnetics*. E.K. Miller, Editor. Van Nostrand Reinhold. New York, pp. 297-351.

Sharma, P. V. 1997. *Environmental and Engineering Geophysics*. Cambridge, UK, Cambridge University Press. 475 pages.

Schwab, G.O., R.K. Frevert, T.W. Edminster, and K.K. Barnes. 1981. *Soil and Water Conservation Engineering,* Third Edition. John Wiley and Sons. New York, 525p.

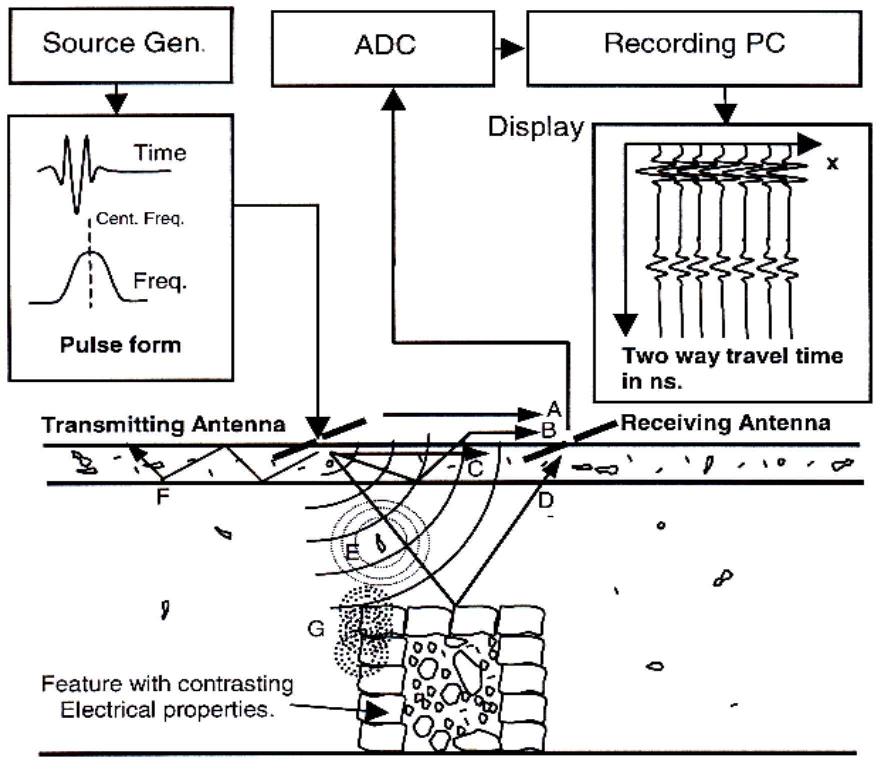

Figure 1. Simplified structural schematic of georadar (GPR)

Figure 2. (GPR) model RAMAC System Set

Table 1. The relative permittivity (εr) and wave velocity

Medium	(εr)	Velocity [m/μs]
Air	1	300
Fresh water	81	33
Limestone	7 - 16	75 - 113
Granite	5 - 7	113 - 134
Schist	5 - 15	77 - 134
Concrete	4 - 10	95 - 150
Clay	4 - 16	74 - 150
Silt	9 - 23	63 - 100
Sand	4 - 30	55 - 150
Moraine	9 - 25	60 - 100
Ice	3 - 4	150 - 173
Permafrost	4 - 8	106 - 150

Table 2. Values of Antenna Frequency, Target Resolution, Depth Estimation, and Depth Maximum Estimation

Antenna Frequency (MHz)	Target Resolution (m)	Depth Estimation (m)	Depth Maximum Estimation (m)
25	1.0	5 – 30	35 - 60
50	0.5	5 – 20	20 - 30
100	0.1 – 1.0	2 - 15	15 - 25
200	0.05 – 0.5	1 - 10	5 - 15
1000	Cm	0.05 - 2	0.5 – 4

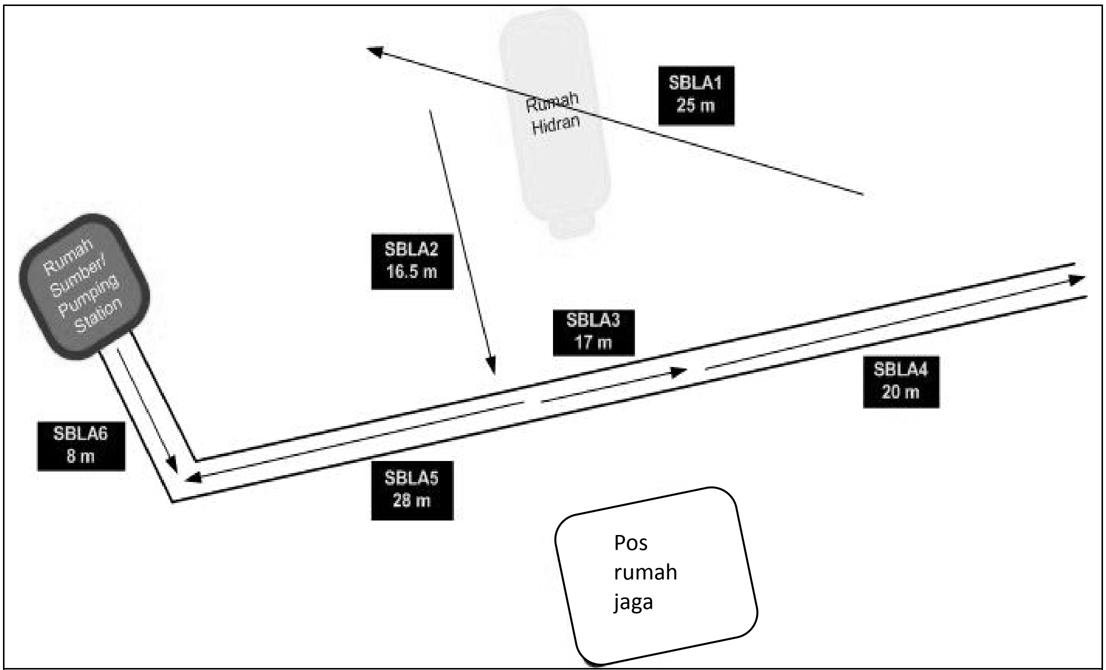

Figure 3a. The 100 MHz GPR antenna survey line lay out

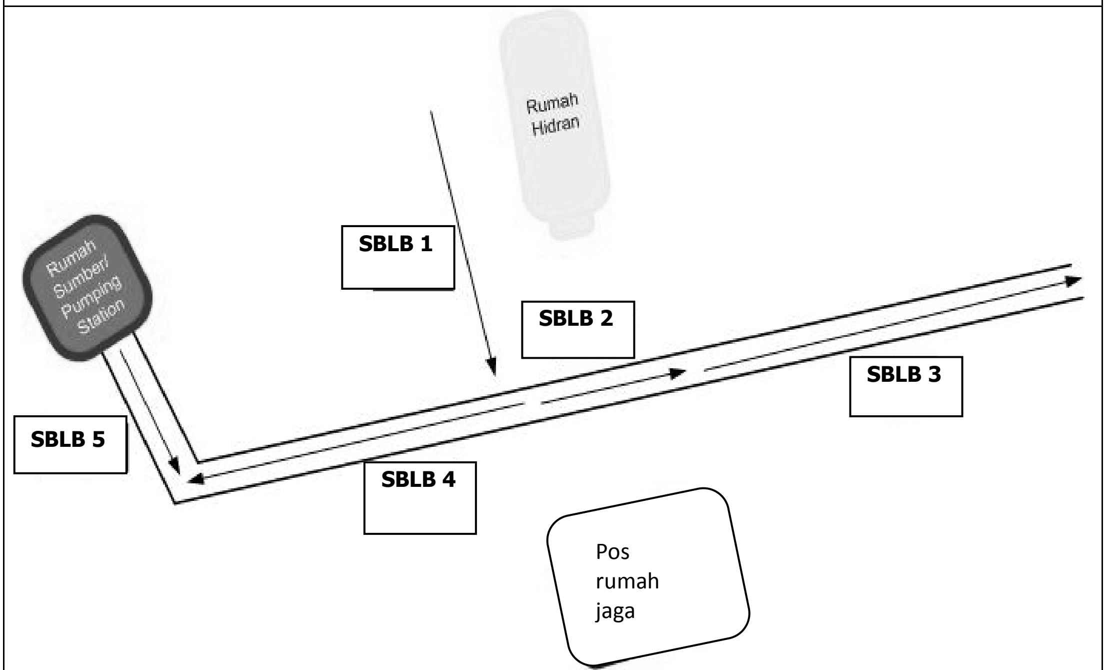

Figure 3b. The 50 MHz GPR antenna survey line lay out

Figure 3. GPR antenna survey line lay out

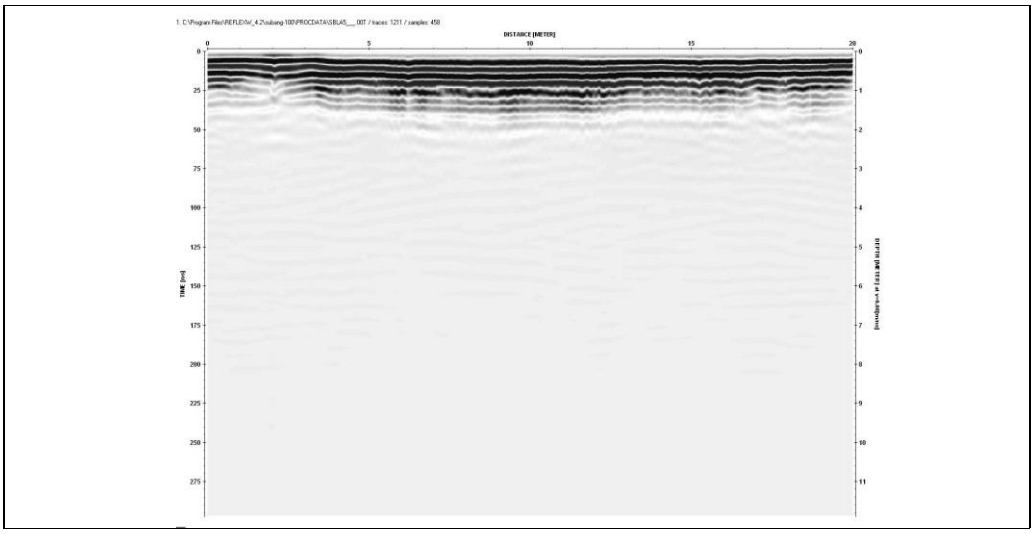

Figure 4. GPR Raw Data

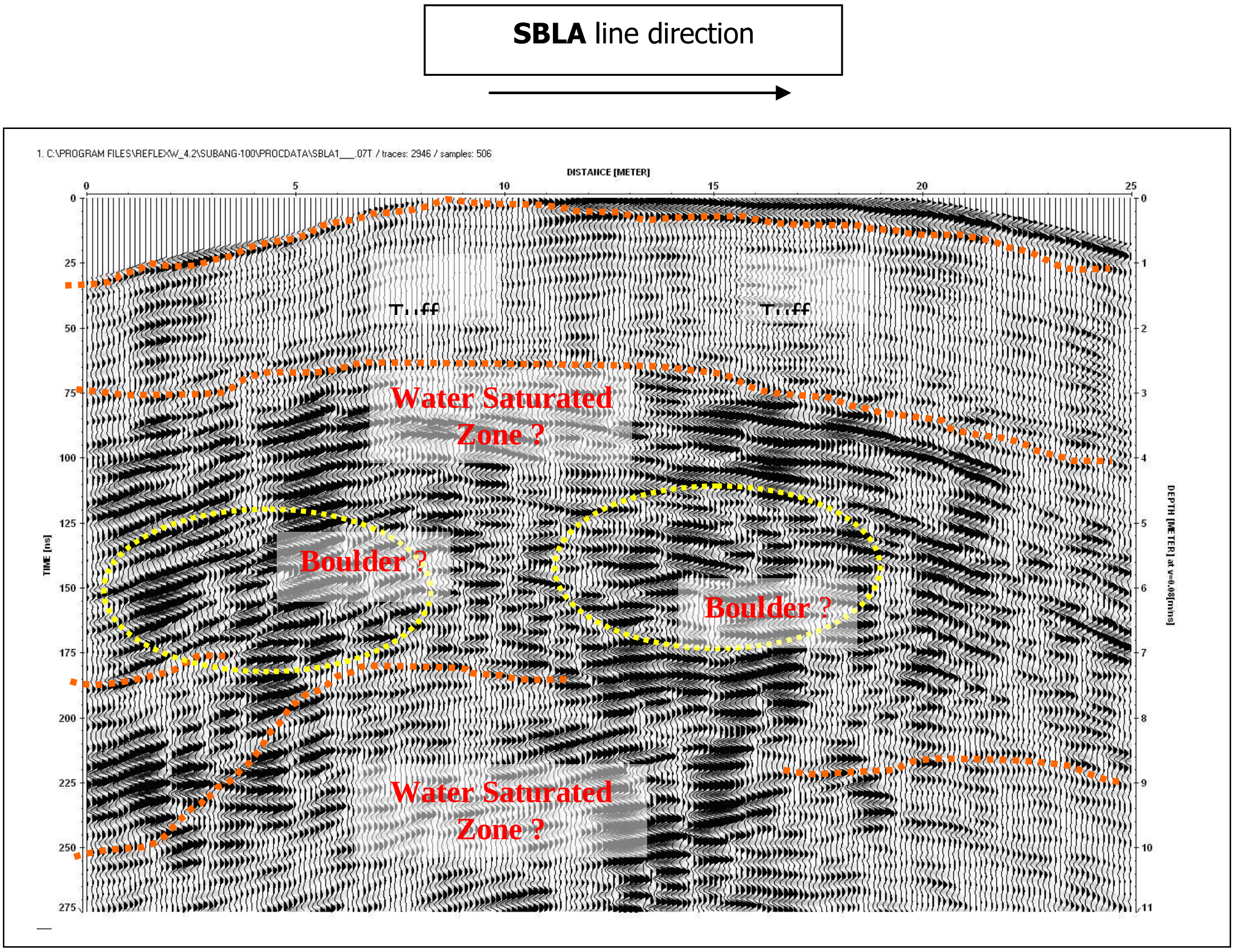

Figure 5a. Radargram from Line SBLA-1 (100 MHz Antenna) GPR survey

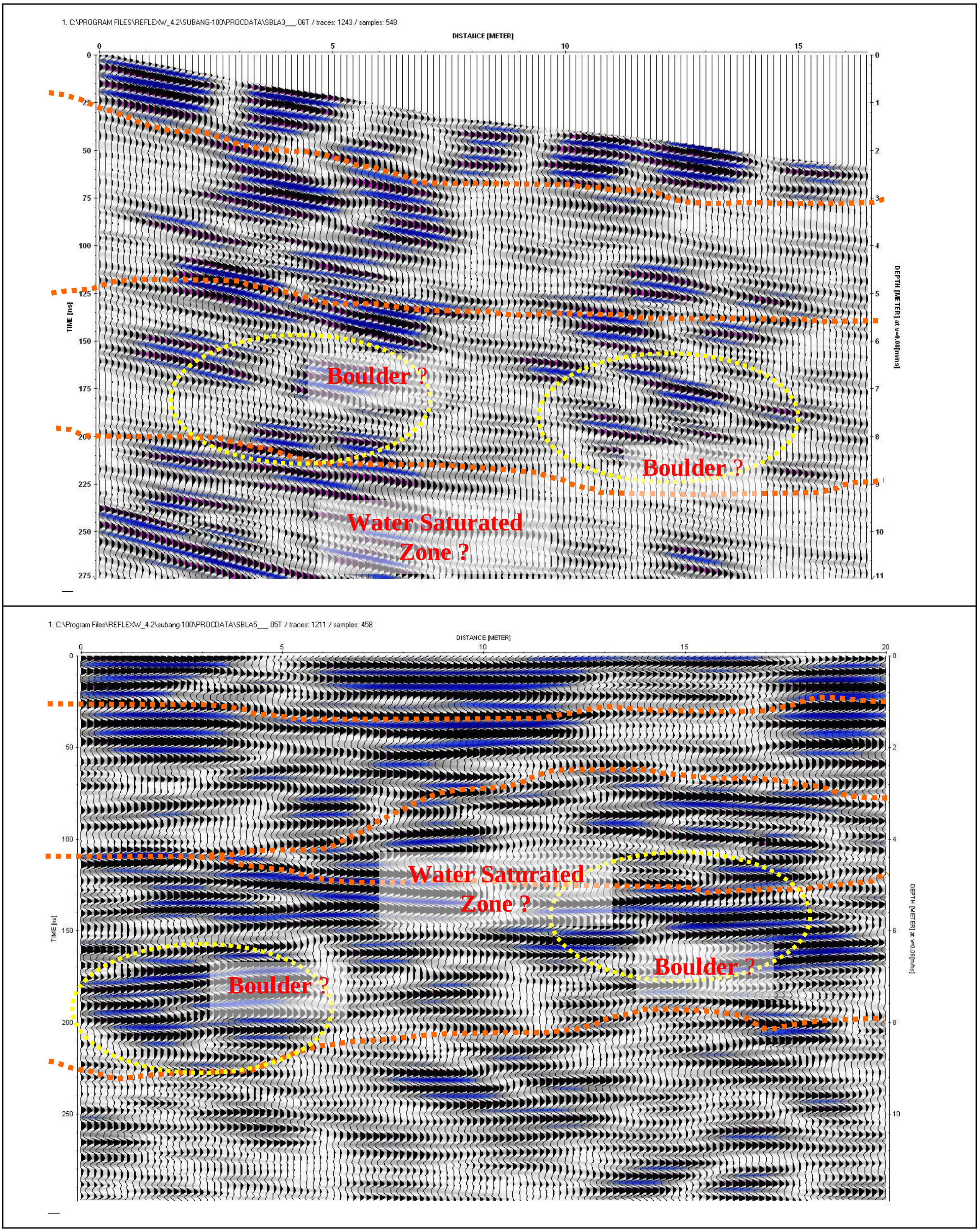

Figure 5b & c. Radargram from Line SBLA-2 and 3 (100 MHz Antenna) GPR survey

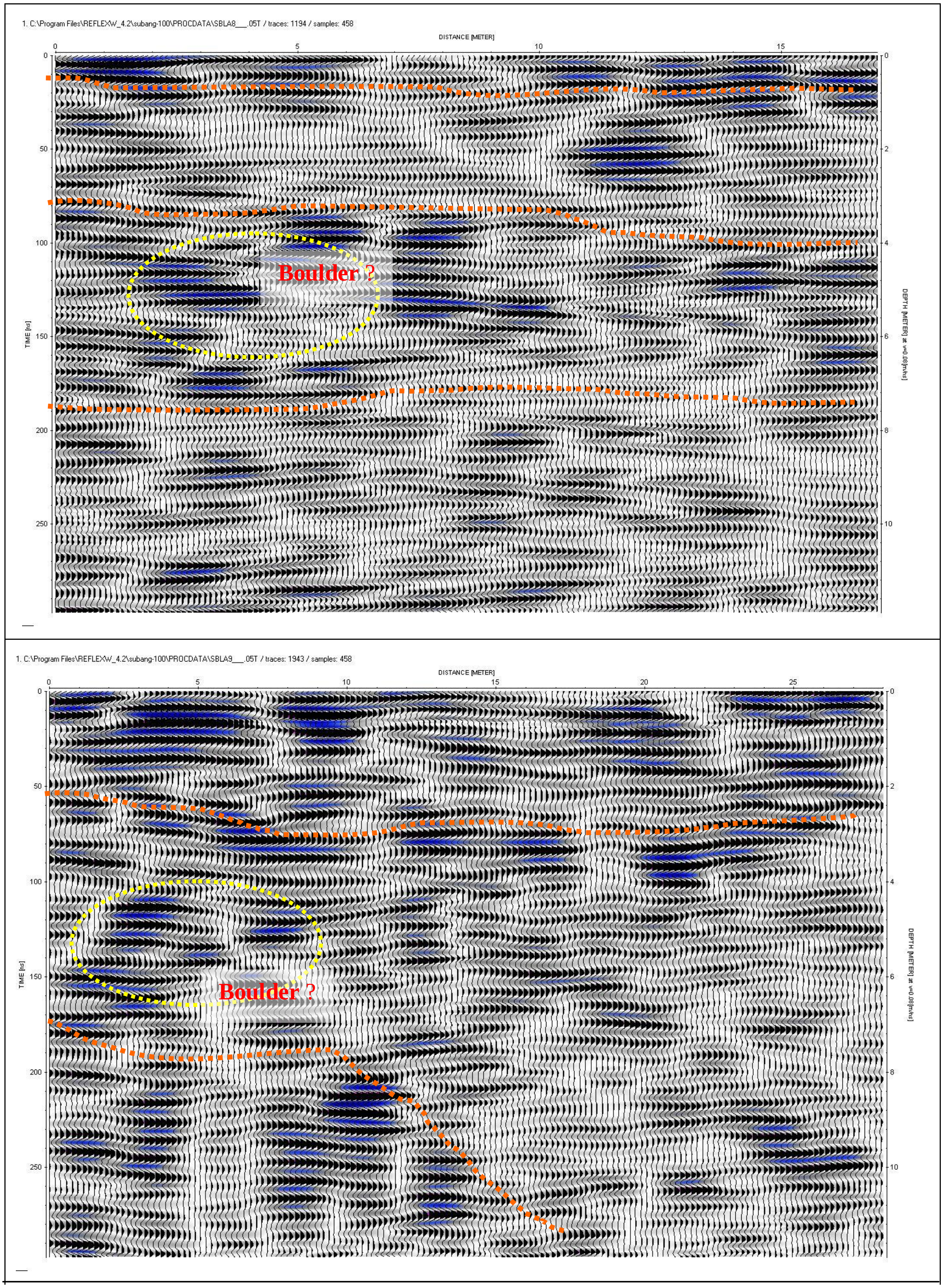

Figure 5d & e. Radargram from Line SBLA-4 and 5 (100 MHz Antenna) GPR survey

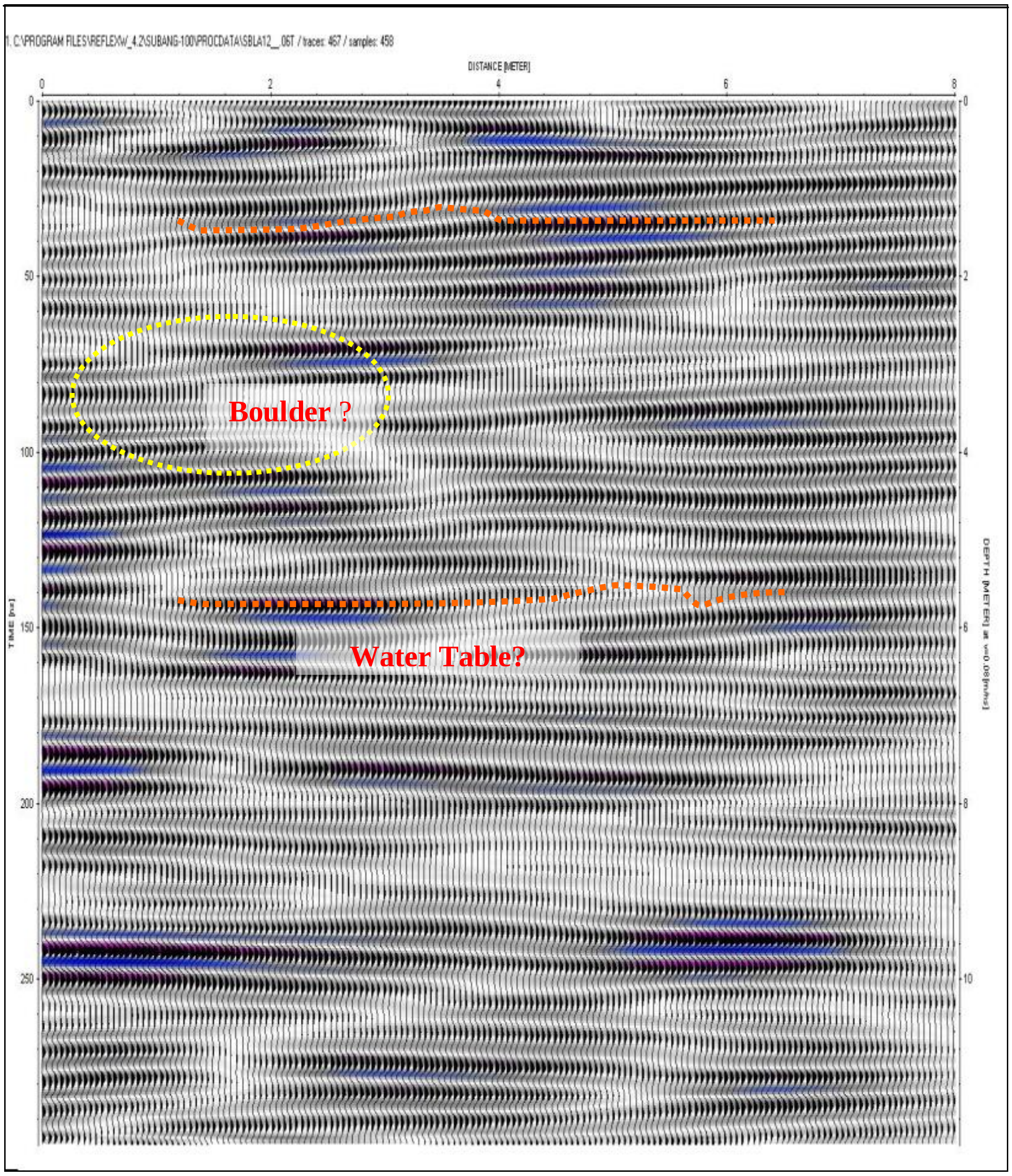

Figure 5f. Radargram from Line SBLA-6 (100 MHz Antenna) GPR survey

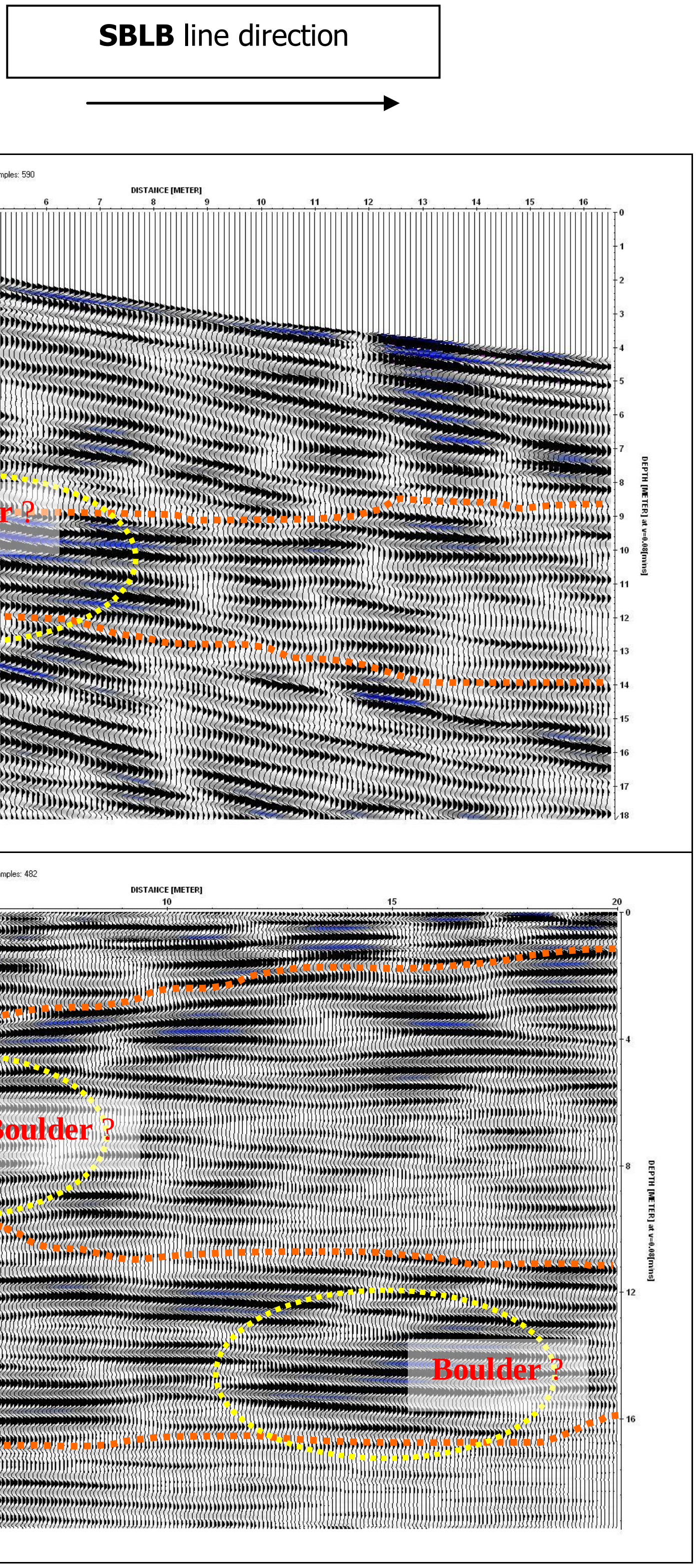

Figure 6a & b. Radargram from Line SBLB1 and 2 (50 MHz Antenna) GPR survey

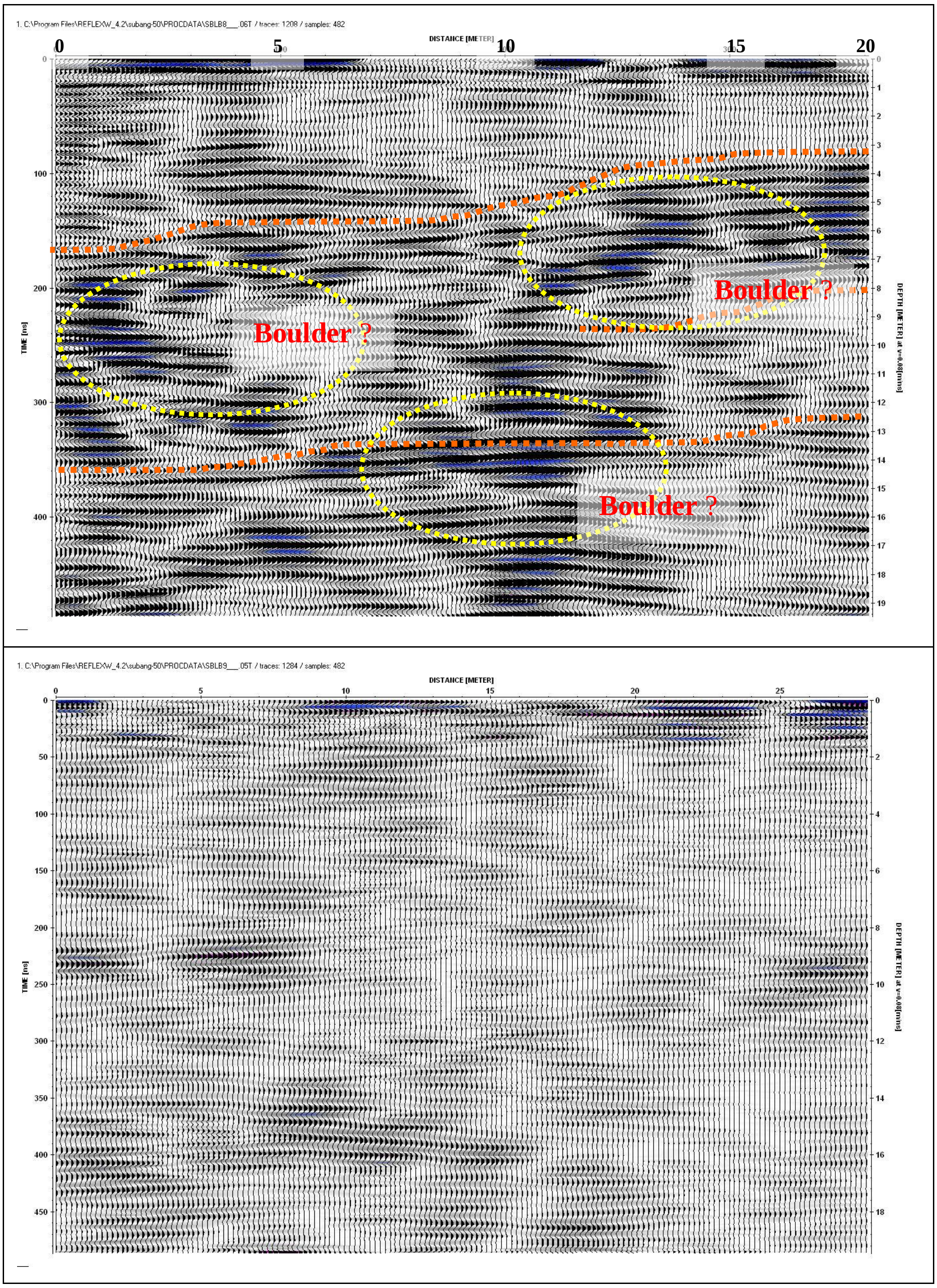

Figure 6c & d. Radargram from Line SBLB-3 and 4 (50 MHz Antenna) GPR survey

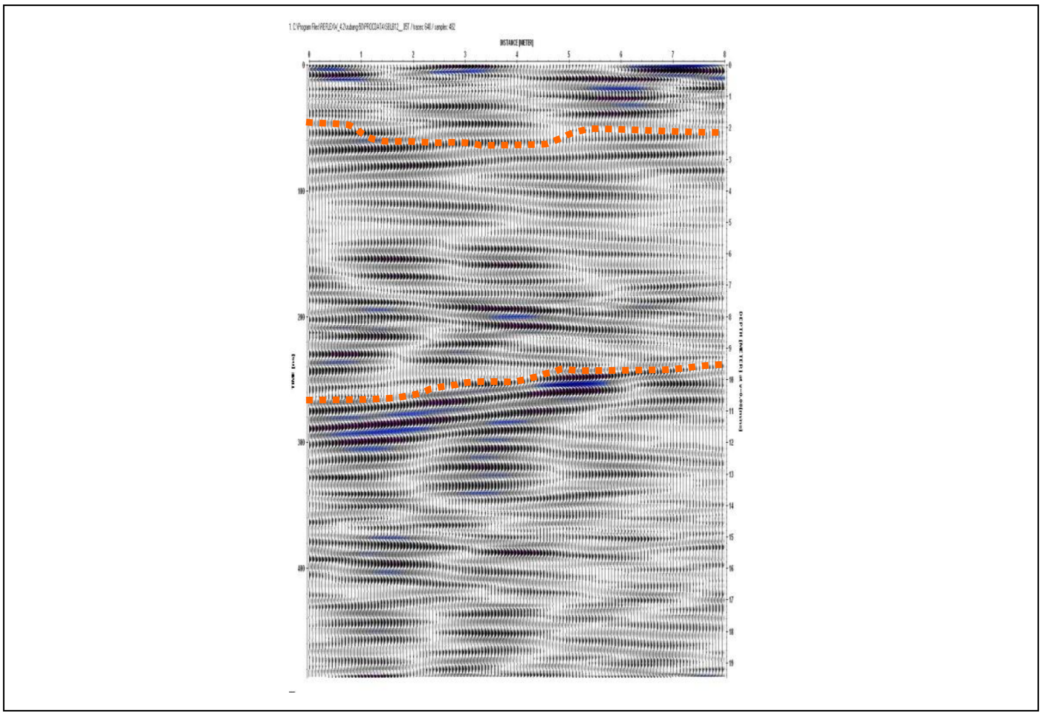

Figure 6e. Radargram from Line SBLB-5 (50 MHz Antenna) GPR survey

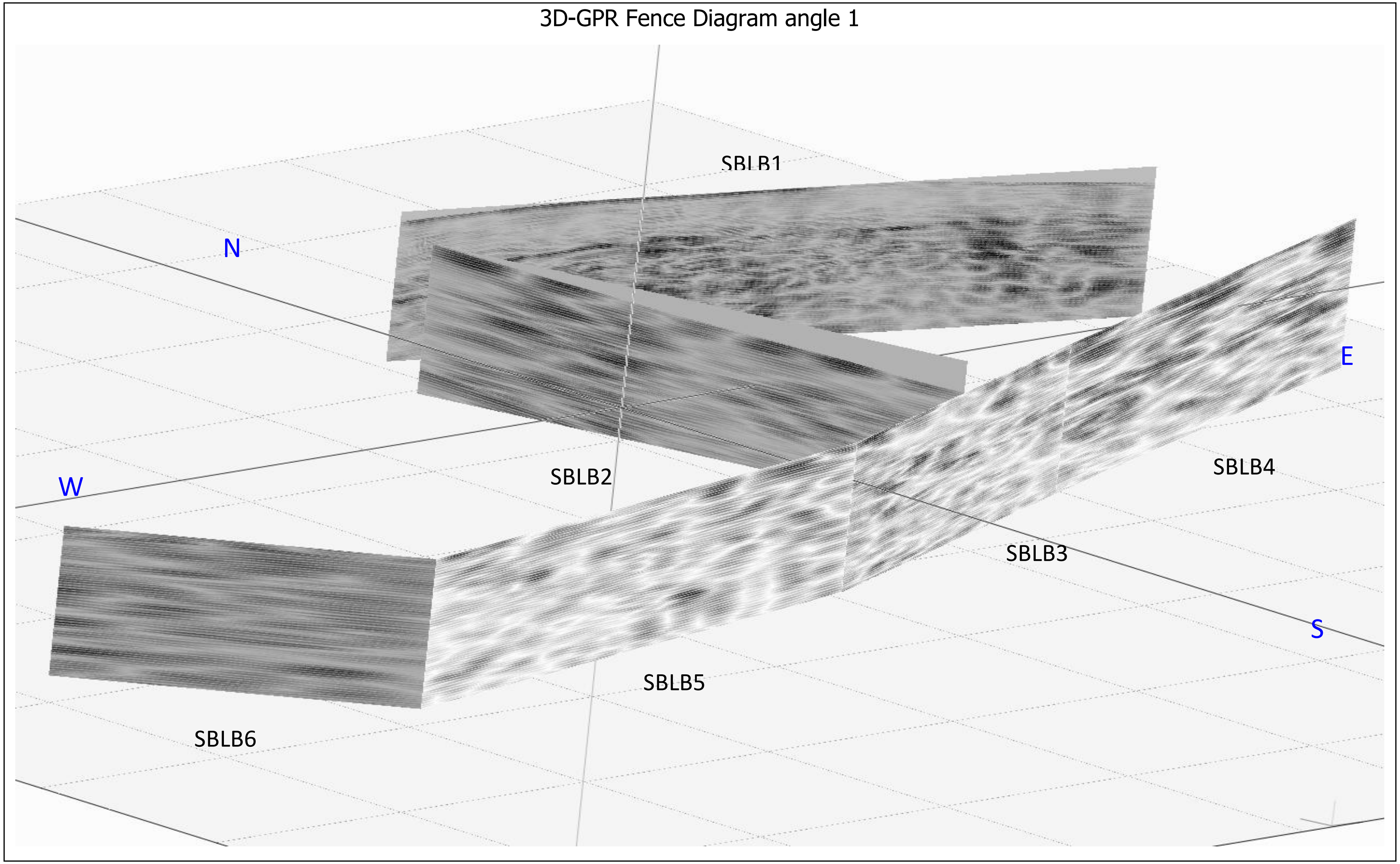

Figure 7. All GPR data line from 100 MHz antenna survey

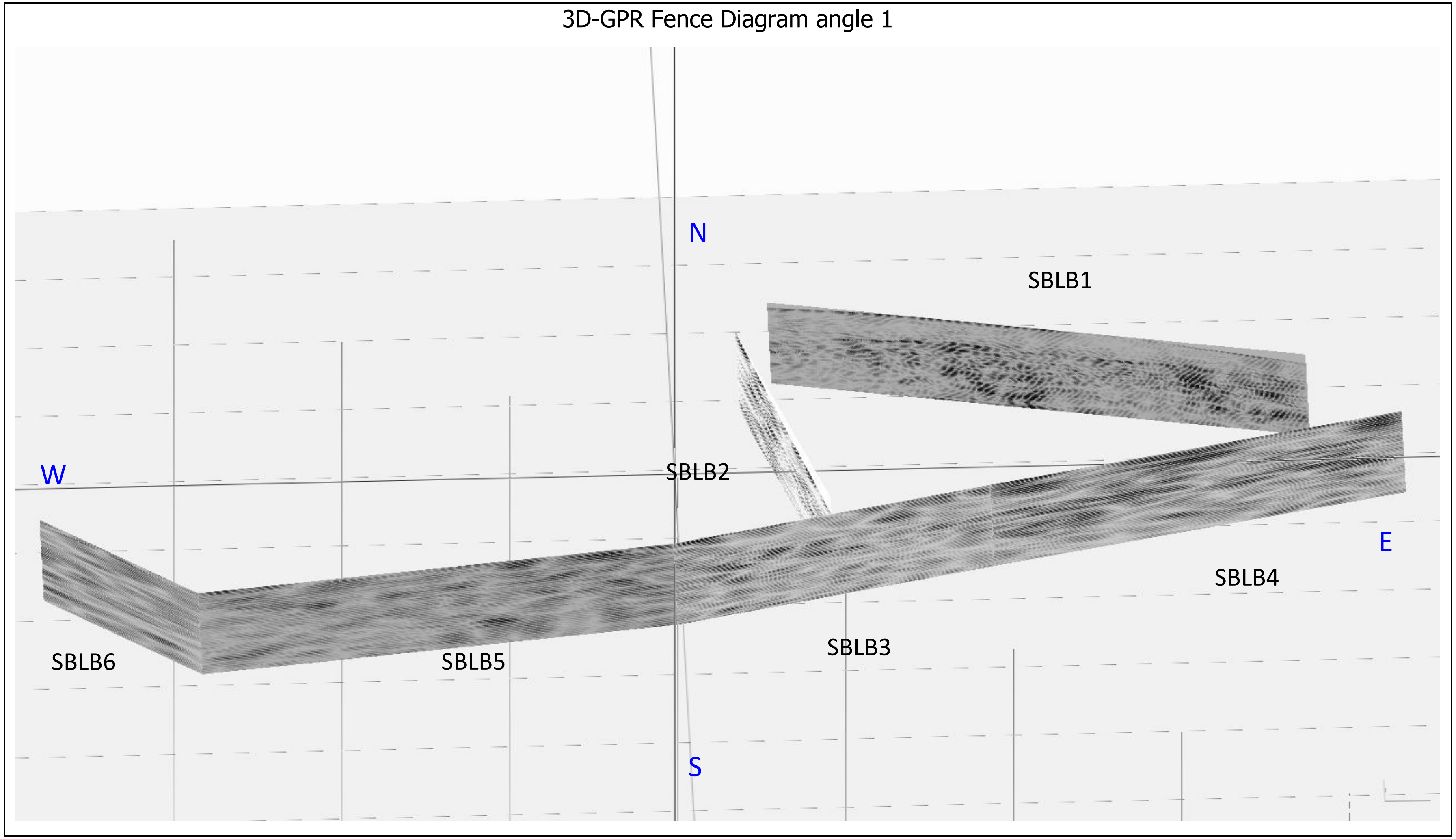

Figure 8. All GPR data line from 100 MHz antenna survey

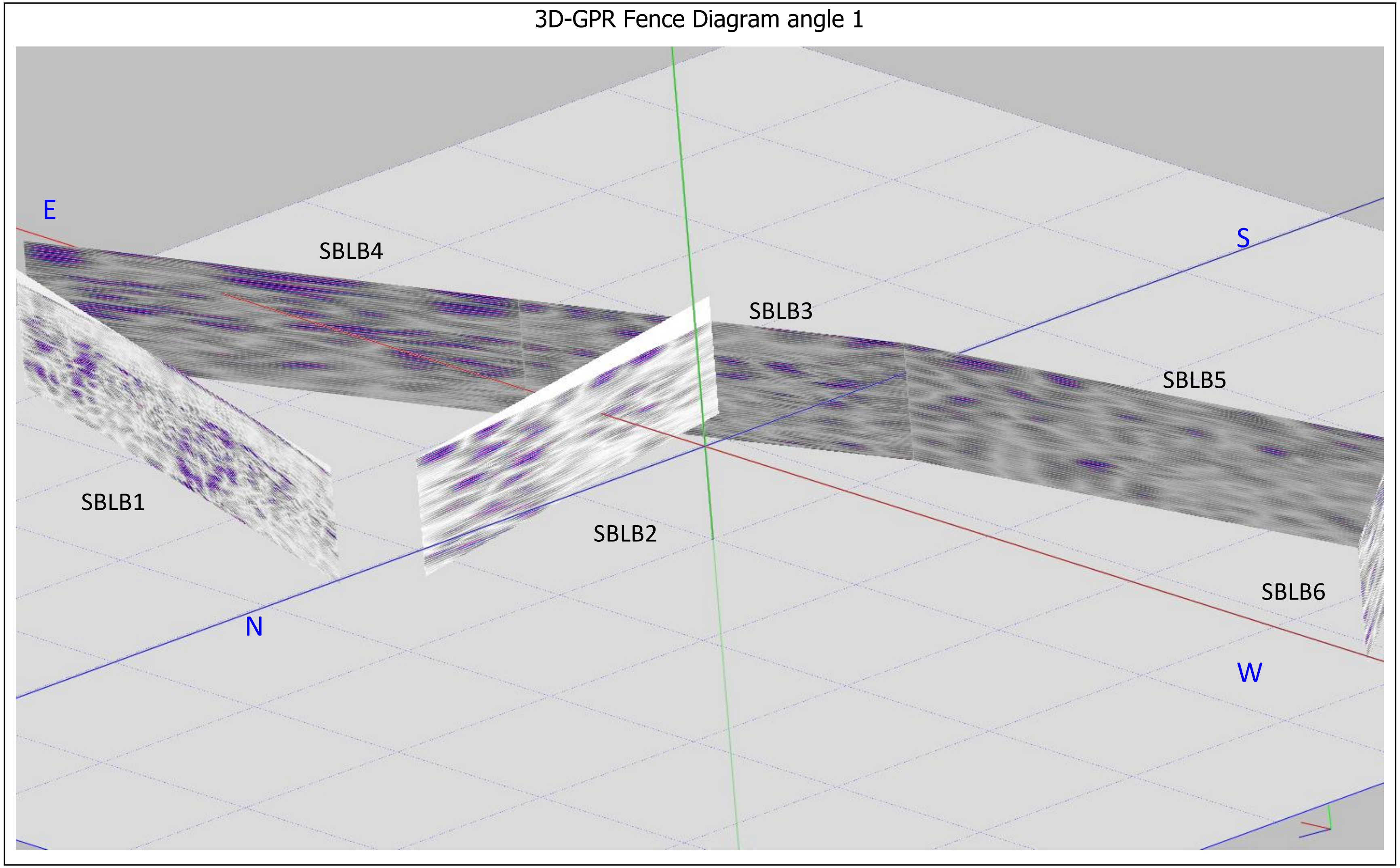

Figure 9. All GPR data line from 100 MHz antenna survey

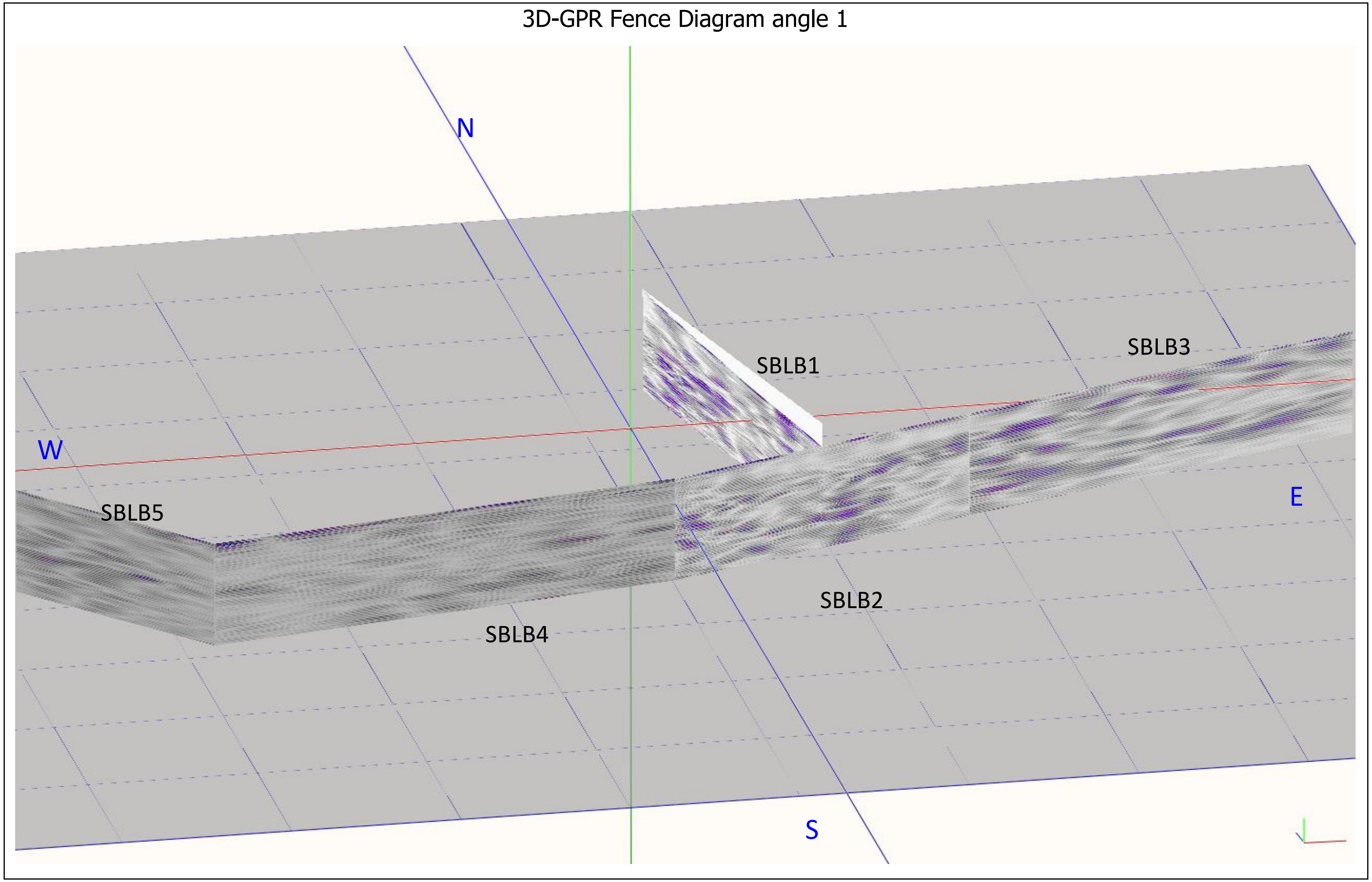

Figure 10. All GPR data line from 50 MHz antenna survey

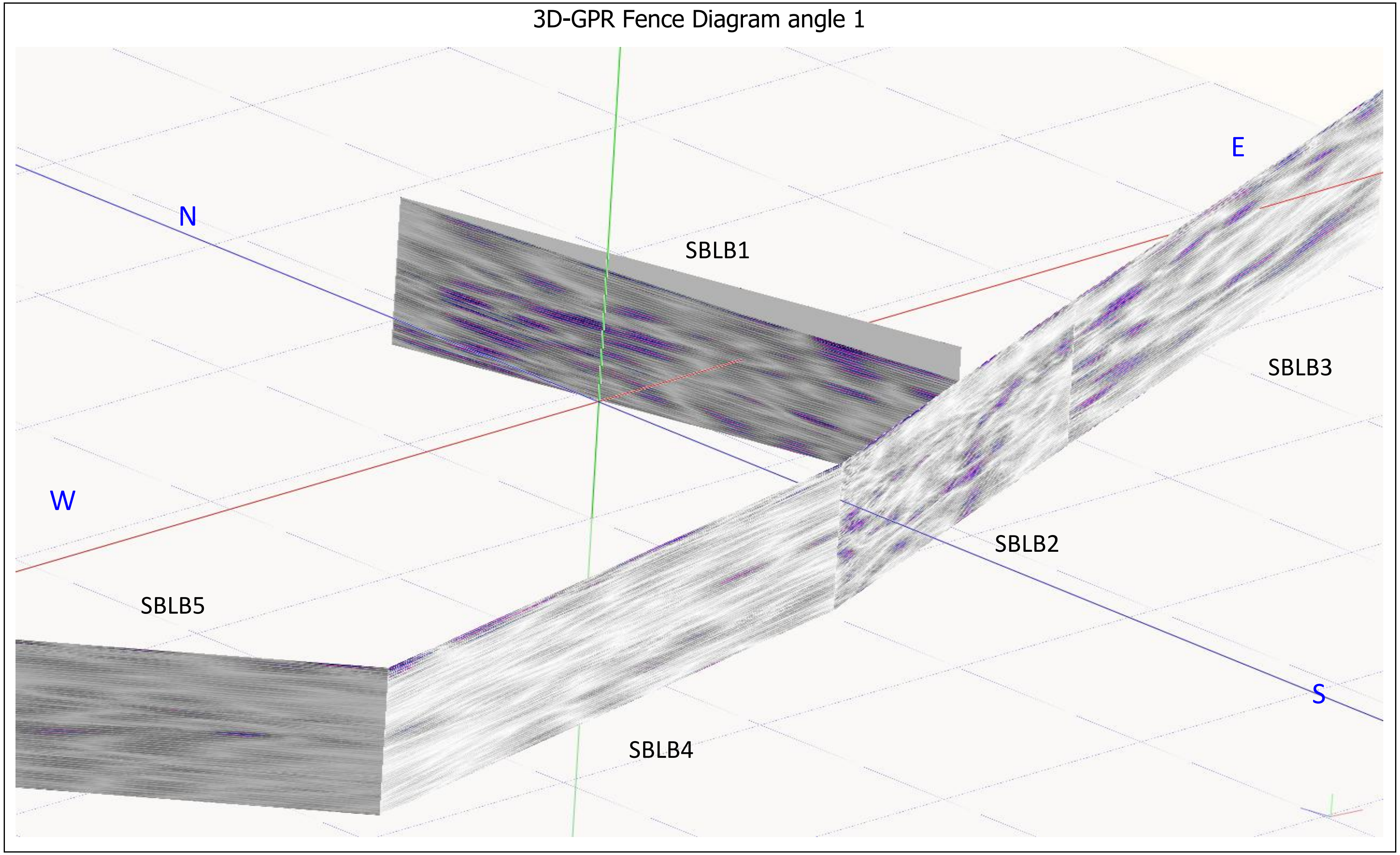

Figure 11. All GPR data line from 50 MHz antenna survey

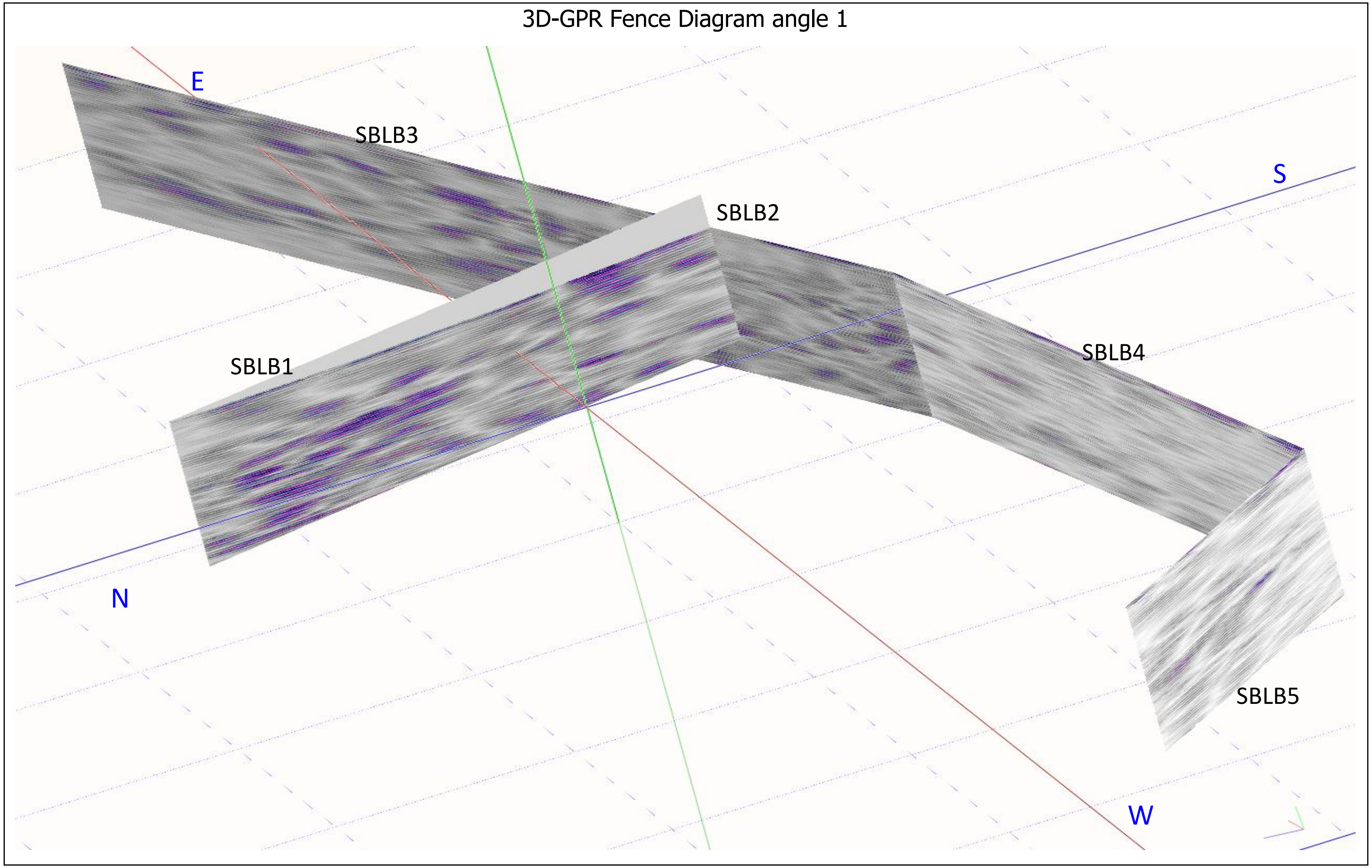

Figure 12. All GPR data line from 50 MHz antenna survey